Electronic supplementary information:

Particle detachment from fluid interfaces: Theory vs. Experiments

Svetoslav E. Anachkov,[‡a,b] Ivan Lesov,[‡a,b] Michele Zanini,[a]
Peter A. Kralchevsky,[b] Nikolai D. Denkov,[b] Lucio Isa*[a]

[a] *Laboratory for Interfaces, Soft matter and Assembly, Department of Materials, ETH Zurich, Vladimir-Prelog-Weg 5, CH-8093 Zurich, Switzerland.*
E-mail: lucio.isa@mat.ethz.ch; Tel: +41 44 633 63 76
[b] *Department of Chemical and Pharmaceutical Engineering, Faculty of Chemistry and Pharmacy, Sofia University, 1 James Bourchier Ave., 1164 Sofia, Bulgaria*
[‡] Both authors contributed equally.

A.1 Comments on GTT for hydrophilic particles

During the experiments we have identified important factors and properties of the gellan gum that affect particle adhesion, thus contact-angle measurement via GTT. This section presents a description of these findings. The physical properties of gellan gum are mainly determined from its major components: high-acyl and low-acyl polysaccharides.[1] The high-acyl polysaccharide sets at 70-80 ºC forming a relatively soft gel. In contrast, the low-acyl polysaccharide sets at 30-50 ºC forming a harder, but less elastic gel. Gellan gums also contain surface-active impurities such as proteins and lipids,[2] which adsorb on both fluid and solid interfaces. Hence, to obtain reliable data for θ using GTT, the gellan gum should be purified.

In our case, the gellan gum was supplied by AppliChem without detailed information for its chemical content. However, from its physical properties, our gellan gum is probably a mixture of both high-acyl and low-acyl polysaccharides. To purify it from surface-active contaminants, we used a high-purity silica gel column (60 Å pores, 70-230 mesh; Fluka, Germany). The purified gellan gum was then used in our GTT experiments.

Our GTT results for non-modified (hydrophilic) silica particles are of particular interest, because they reveal why GTT often provides higher values for θ than FreSCa. The reason for this difference is the following: the most hydrophilic particles remain embedded in the gellan gum after the PDMS replica is peeled off, and therefore they are missing in the final contact-angle distribution. To understand this effect, we will compare the adhesion energies silica-to-gellan-gum, E_{SG}, and silica-to-PDMS, E_{SP}, which can be calculated as follows:

$$E_{SG} = \gamma_{SG} S_{SG} = 2\pi R^2 \gamma_{SG} (1 + \cos\theta), \tag{A.1}$$

$$E_{SP} = \gamma_{SP} S_{SP} = 2\pi R^2 \gamma_{SP} (1 - \cos\theta), \tag{A.2}$$

where γ_{SG} and γ_{SP} are the respective adhesion energies per unit area. For a given particle, S_{SG} is the contact area with the gellan gum, whereas S_{SP} is the contact area with the PDMS. It is useful to recast eqn (A.1) and (A.2) in dimensionless form:

$$\varepsilon_{SG} \equiv \frac{E_{SG}}{4\pi R^2 \gamma_{SG}} = \frac{1+\cos\theta}{2} = \cos^2\frac{\theta}{2}, \tag{A.3}$$

$$\varepsilon_{SP} \equiv \frac{E_{SP}}{4\pi R^2 \gamma_{SG}} = \frac{\gamma_{SP}}{\gamma_{SG}}\frac{1-\cos\theta}{2} = \frac{\gamma_{SP}}{\gamma_{SG}}\sin^2\frac{\theta}{2}. \tag{A.4}$$

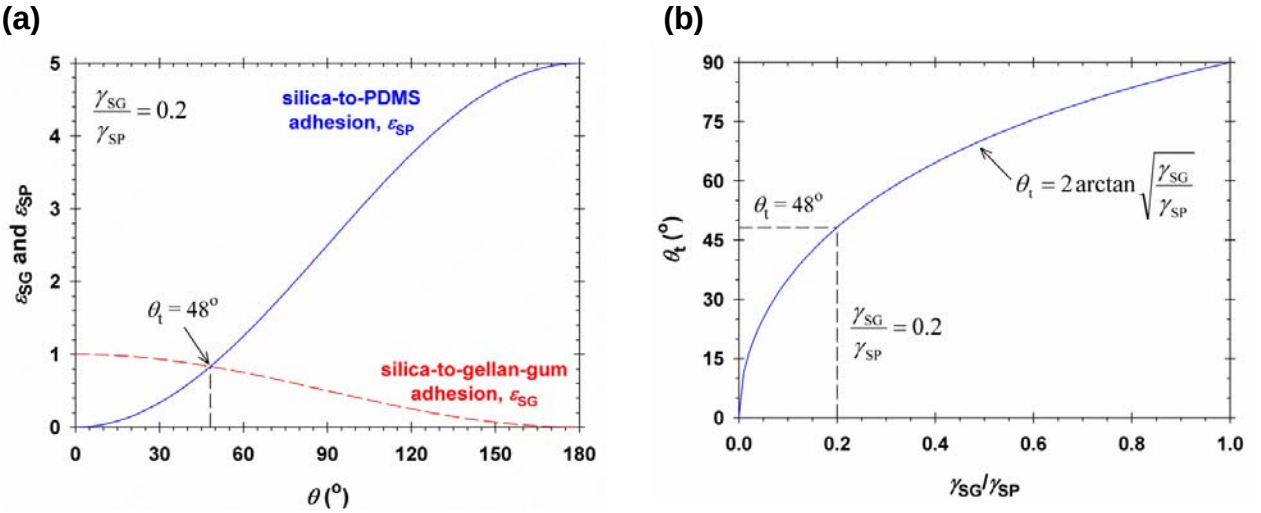

Fig. A1 (a) Plots of the dimensionless adhesion energies silica-to-gellan-gum ε_{SG} (dashed line) and silica-to-PDMS ε_{SP} (solid line) versus θ. ε_{SG} and ε_{SP} are calculated from eqn (A.3) and (A.4), having $\gamma_{SG} / \gamma_{SP} = 0.2$. (b) Plot of the threshold contact angle θ_t as a function of $\gamma_{SG} / \gamma_{SP}$.

Here, ε_{SG} and ε_{SP} are the dimensionless energies for silica-to-gellan-gum and silica-to-PDMS adhesion. ε_{SG} decreases with the contact angle θ, whereas ε_{SP} increases with θ (Fig. A1a). In the case of very hydrophilic particles, θ approaching 0º, the particles are fully-embedded in the gellan gum and $\varepsilon_{SP} = 0$. In the case of superhydrophobic particles, θ approaching 180º, the particles are fully-embedded in the PDMS and $\varepsilon_{SG} = 0$. There is a threshold contact angle, θ_t, for which:

$$E_{SG} = E_{SP} \Leftrightarrow \varepsilon_{SG} = \varepsilon_{SP}. \tag{A.5}$$

Substituting eqn (A.3) and (A.4) into eqn (A.5), we have:

$$\tan^2\frac{\theta_t}{2} = \frac{\gamma_{SG}}{\gamma_{SP}} \Leftrightarrow \theta_t = 2\arctan\sqrt{\frac{\gamma_{SG}}{\gamma_{SP}}}. \tag{A.6}$$

Fig. A1b shows that θ_t increases as a function of $\gamma_{SG} / \gamma_{SP}$. As expected, for $\gamma_{SG} / \gamma_{SP} = 1$, $\theta_t = 90^o$. For $\theta < \theta_t$, the particles are expected to be trapped predominantly in the gellan gum.

These theoretical predictions were confirmed experimentally. Indeed, the most hydrophilic silica particles (35° ± 9°) were trapped in the gellan gum, thus leaving holes in the PDMS replica; see Fig. A2a. The remaining particles (51° ± 7°) were embedded in the PDMS; see Fig. A2b. The threshold contact angle θ_t should be around 43° (the average of 35° and 51°), meaning that $\gamma_{SG} / \gamma_{SP} \approx 0.16$. To decrease θ_t and entrap even the most hydrophilic particles, we used a UV-glue replica instead of a PDMS one, as reported in the main body of the manuscript. The former adheres to silica more strongly than the latter; hence, very few particles are left in the gellan gum and a more faithful representation of the contact angle distribution is found.

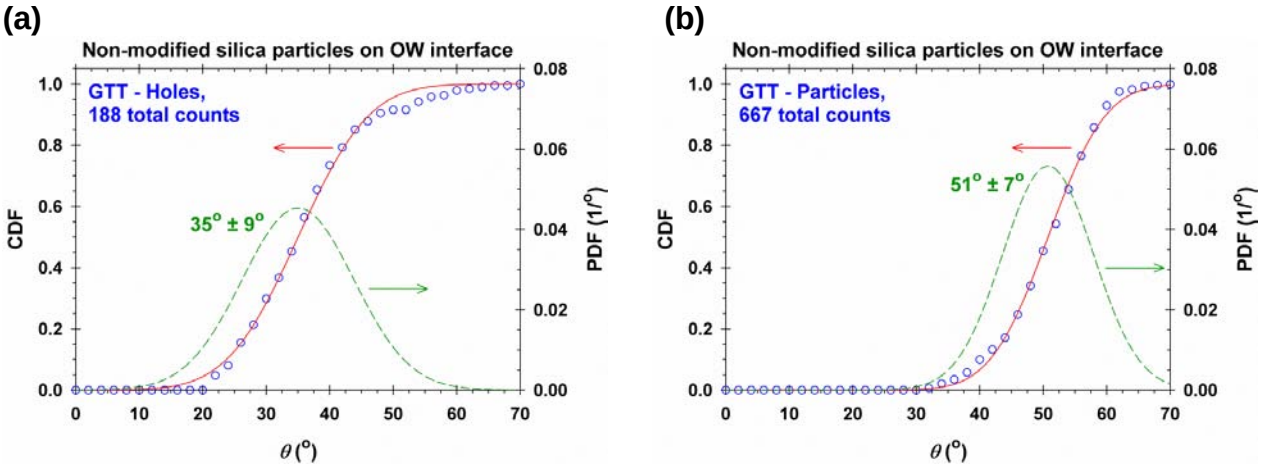

Fig. A2 Three-phase contact angle distributions of non-modified silica particles at the oil-water (OW) interface. The distributions in terms of CDF (solid line) and PDF (dashed line) are calculated after statistical analysis of our experimental data (empty circles) from the gel-trapping technique (GTT). Using GTT, we obtained the contact-angle distributions from (a) holes left in the PDMS and from (b) silica particles embedded in the PDMS.

A.2 Error estimates for θ determined from AFM measurements

The contact angle θ of a smooth solid microsphere attached to a fluid interface can be determined by analyzing the force-distance curves measured upon particle approach and retraction via colloidal-probe AFM. From the experimental data, we directly extract: (i) the jump-in distance δ; (ii) the maximal force for particle detachment F_{max}; (iii) the work of the capillary force W; and (iv) the maximal detachment distance D_{max}. All these physical parameters, however, are measured with inherent experimental errors, which lead to uncertainties $\Delta\theta$ in the contact-angle determination.

In general, these experimental errors are relatively small and can be connected to $\Delta\theta$ as follows:

$$\Delta\psi(\theta,\alpha,\varepsilon) = \psi(\theta+\Delta\theta,\alpha,\varepsilon) - \psi(\theta,\alpha,\varepsilon) \approx \frac{d\psi}{d\theta}\Delta\theta, \tag{A.7}$$

where $\psi(\theta, \alpha, \varepsilon)$ denotes an experimental parameter, which depends on $\theta, \alpha, \varepsilon$. All angles are expressed in radians and $\Delta\theta$ is considered to be a small parameter. From eqn (A.7), we can derive the formula for the absolute value of $\Delta\theta$, which reads:

$$\Delta\theta = \frac{\Delta\psi}{\left|d\psi/d\theta\right|} = \frac{\psi}{\left|d\psi/d\theta\right|}\frac{\Delta\psi}{\psi}. \tag{A.8}$$

Using eqn (2), (22) and (A.8), $\Delta\delta$ and $\Delta F_{\max}$ are related to $\Delta\theta_\delta$ and $\Delta\theta_f$ as follows:

$$\Delta\theta_\delta = \frac{1}{\sin\theta}\frac{\Delta\delta}{R} = \frac{1+\cos\theta}{\sin\theta}\frac{\Delta\delta}{\delta} = \cot\frac{\theta}{2}\frac{\Delta\delta}{\delta}, \tag{A.9}$$

$$\Delta\theta_f = \frac{2}{\sin\theta}\frac{\Delta F_{\max}}{2\pi R\sigma} = \frac{2\cos^2\frac{\theta}{2}}{\sin\theta}\frac{\Delta F_{\max}}{F_{\max}} = \cot\frac{\theta}{2}\frac{\Delta F_{\max}}{F_{\max}}. \tag{A.10}$$

Eqn (A.9) and (A.10) both have exactly the same prefactor multiplying $\Delta\delta/\delta$ and $\Delta F_{\max}/F_{\max}$. In Fig. A3a, these formulae, eqn (A.9) and (A.10), are compared to the exact numerical calculations for $\Delta\theta_\delta$ and $\Delta\theta_f$. From the comparison, we see that eqn (A.9) and (A.10) hold for $\Delta\theta < 10°$ and $\theta > 57°$, where the difference between analytical and numerical calculations is less than 5 %.

In analogous way, using eqn (3), (7) and (A.8), $\Delta D_{\max}$ and ΔW can be related to $\Delta\theta_d$ and $\Delta\theta_w$. For simplicity, $\Delta\theta_d$ and $\Delta\theta_w$ are both evaluated using $\alpha_{\max,1} = (\pi+\theta)/2$ as an approximation for $\alpha_{\max,2}$:

$$\Delta\theta_d = \frac{2}{\sin\theta}\frac{1}{1-\ln\left[\frac{\varepsilon}{4}\cos\frac{\theta}{2}\left(1+\sin\frac{\theta}{2}\right)\right]-\gamma_e}\frac{\Delta D_{\max}}{R}, \tag{A.11}$$

$$\Delta\theta_d = \cot\frac{\theta}{2}\frac{\Delta D_{\max}}{D_{\max}}, \quad \varepsilon << 1 \tag{A.12}$$

$$\Delta\theta_w = \frac{4}{\sin^3\theta}\frac{\sin^2\frac{\theta}{2}\left(1+\sin\frac{\theta}{2}\right)}{\left(1+\sin\frac{\theta}{2}\right)\left(3-\ln\left[\frac{\varepsilon}{4}\cos\frac{\theta}{2}\left(1+\sin\frac{\theta}{2}\right)\right]-\gamma_e\right)-2}\frac{\Delta W}{\pi R^2\sigma}, \tag{A.13}$$

$$\Delta\theta_w = \frac{1}{2}\cot\frac{\theta}{2}\frac{\Delta W}{W}, \quad \varepsilon << 1. \tag{A.14}$$

For small particles with $\varepsilon < 10^{-2}$, eqn (A.11) and (A.13) transform into eqn (A.12) and (A.14), respectively. Eqn (A.12) has exactly the same prefactor as in eqn (A.9) and (A.10), whereas the prefactor in eqn (A.14) is two times smaller. In Fig. A3b and A3c, the analytical expressions, eqn (A.12) and (A.14), are compared to the exact numerical calculations. The comparisons show

that eqn (A.12) is valid for $\Delta\theta < 12°$ and $\theta > 48°$, whereas eqn (A.14) is applicable for $\Delta\theta < 9°$ and $\theta > 33°$.

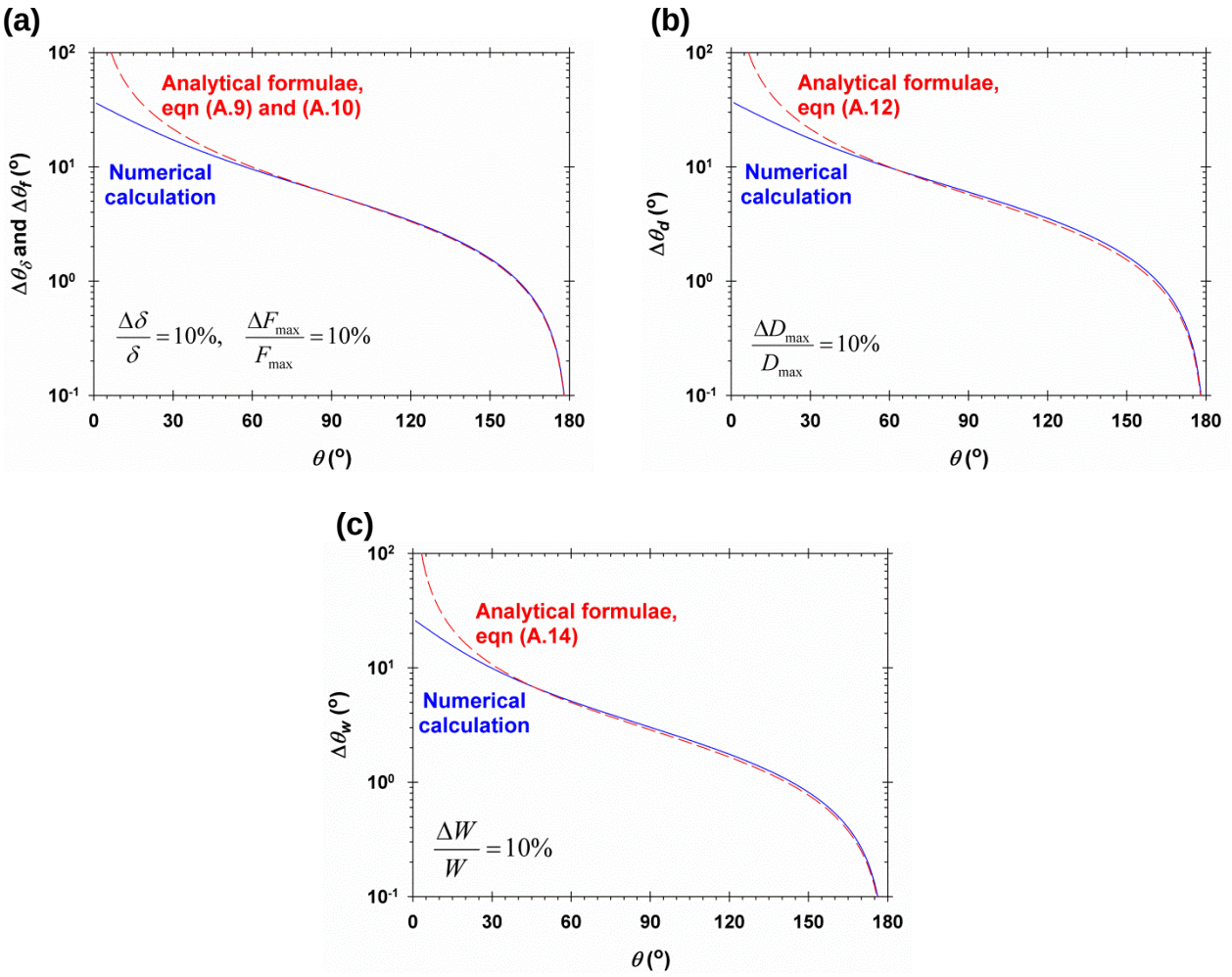

Fig. A3 The absolute contact-angle uncertainties (a) $\Delta\theta_\delta$ and $\Delta\theta_f$, (b) $\Delta\theta_d$ and (c) $\Delta\theta_w$ are plotted as a function of θ. They are all calculated for 10 % relative error of the respective physical parameter. The analytical evaluations are represented as dashed lines, whereas the exact numerical calculations are depicted as solid lines.

References

1 KELCOGEL® Gellan Gum Book, CP Kelco, USA, 2007, 5th edition.

2 V. N. Paunov, *Langmuir*, 2003, **19**, 7970–7976.